

Analyzing Eye Tracking Data in Mirror Exposure

Nina Döllinger
PIIS Group, University of Würzburg
Würzburg, Germany
nina.doellinger@uni-wuerzburg.de

Christopher Göttfert
PIIS Group, University of Würzburg
Würzburg, Germany
christopher.goettfert@uni-wuerzburg.de

Erik Wolf
HCI Group, University of Würzburg
Würzburg, Germany
erik.wolf@uni-wuerzburg.de

David Mal
HCI Group, University of Würzburg
Würzburg, Germany
david.mal@uni-wuerzburg.de

Marc Erich Latoschik
HCI Group, University of Würzburg
Würzburg, Germany
marc.latoschik@uni-wuerzburg.de

Carolin Wienrich
PIIS Group, University of Würzburg
Würzburg, Germany
carolin.wienrich@uni-wuerzburg.de

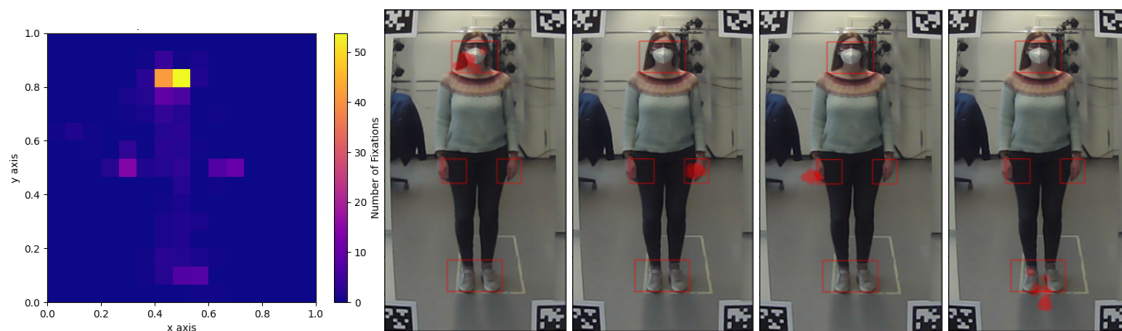


Figure 1: Heat map of fixations (left) and reference picture, calculated AoI bounding boxes and fixations during guided mirror exposure created from our framework (from left to right: head, left hand, right hand, feet).

ABSTRACT

Mirror exposure is an important method in the treatment of body image disturbances. Eye tracking can support the unaffected assessment of attention biases during mirror exposure. However, the analysis of eye tracking data in mirror exposure comes with various difficulties and is associated with a high manual workload during data processing. We present an automated data processing framework that enables us to determine any body part as an area of interest without placing markers on the bodies of participants. A short, formative user study proved the quality compared to the gold standard. The automatic processing and openness for different systems allow a broad range of applications.

CCS CONCEPTS

• **Human-centered computing** → **Virtual reality**; Laboratory experiments; Heat maps; Information visualization.

KEYWORDS

gaze detection, eye tracking, mirror exposure, area of interest

ACM Reference Format:

Nina Döllinger, Christopher Göttfert, Erik Wolf, David Mal, Marc Erich Latoschik, and Carolin Wienrich. 2022. Analyzing Eye Tracking Data in Mirror Exposure. In *Mensch und Computer 2022 (MuC '22)*, September 4–7, 2022, Darmstadt, Germany. ACM, New York, NY, USA, 5 pages. <https://doi.org/10.1145/3543758.3547567>

1 INTRODUCTION

Mirror exposure, the prolonged confrontation with one's mirror image, is a well-known method in the treatment of body dysmorphic or eating disorders. It helps reduce symptoms of body image disturbance, the "excessively negative, distorted, or inaccurate perception of one's own body or parts of it" [19, MB27.3], by reducing attention biases and dissatisfaction towards specific body parts [7]. To understand the underlying effects of mirror exposure, research on body image disorders has repeatedly examined the visual attention bias when looking at one's own body. As the assessment of attention bias via self-report is often biased, indirect methods of measuring attention such as eye tracking can support the analysis of mirror exposure and tracking of changes over time. Combined with methods like thinking aloud and body part ranking according to their perceived attractiveness, eye tracking helps identify an attention bias towards specific body regions [15]. Various eye tracking studies have shown that, particularly in the field of eating disorders, the gaze behavior on the own body is biased [1, 2, 9, 15]. When confronted with photographs of their body, individuals with eating disorders tend to focus predominantly on body parts they

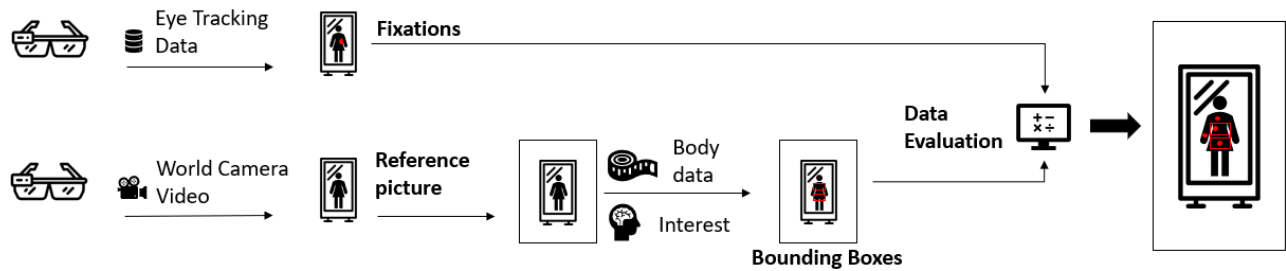


Figure 2: Processing steps of the framework. Upper path: Extraction of Fixations from eye tracking data. Lower path (from left to right): Creating a Reference Picture from world camera video, Definition of AoI and bounding boxes from body data. Final step: Combining fixations and bounding boxes for Data Evaluation.

find unattractive or unsatisfactory [2]. However, the analysis of eye tracking data in mirror exposure comes with a variety of difficulties. In contrast to the processing of gaze behavior on a computer screen, it is not easily possible to automatically define individual body parts as Areas of Interest (AoI) on a mirror.

In eye tracking scenarios without computer screen, one possibility to define AoI is to use tracking markers [17]. However, compared to other scenarios, it is challenging to use tracking markers to indicate body parts as AoI. Attaching them to the body could be perceived as intrusive by the individuals, particularly when the body perception is distorted. Further, idle body movements during mirror exposure complicate the definition of AoI due to varying rotation angles between markers. Hence, most studies present pictures of the participants' body or body parts on a computer monitor to investigate the attention bias [1, 2, 12]. The combination of mirror exposure and eye tracking is rare [7].

Tuschen-Caffier et al. [15] presented a study on attention bias towards disliked body parts that combined mirror exposure with eye tracking. However, their data processing was performed manually, identifying body parts, AoI, and fixations frame by frame. Similarly, Naumann et al. [9] investigated the effect of happiness and sadness on the attention bias using eye tracking in a mirror exposure task. Here too, the data processing was performed manually, using a reference picture instead of the video footage to define fixations.

In sum, past work showed the importance and effectiveness of mirror exposure for body distortion treatments. Eye tracking can support the unaffected assessment of the attention bias but is mainly measured on photographs or computer screens and not in combination with the real-time mirror exposure. If combined, the data analysis was carried out manually in a very laborious-intensive, time-consuming process. So far, no solution has been presented for automatic analysis and evaluation of eye tracking data in mirror exposure.

In our approach, we present an automated data processing framework that enables to determine any body part as AoI, without placing markers on the bodies of our participants. We support our framework with a short, formative user study in which we compare automatically created AoI to the previous gold standard, i.e., manually adjusted AoI. Thus, the present work contributes to an improvement and dissemination of the effortful mirror exposure.

2 SYSTEM DESCRIPTION

2.1 Hardware and Software

As an eye tracking device, we used the Pupil Core¹ glasses by Pupil Labs [8]. It includes two eye cameras recording the eye movements (refresh rate of 200 Hz) and one world camera recording the user's field of view (refresh rate set to 120 Hz). The Pupil Core advertises an accuracy of 0.6° and a precision of 0.02°. We connected the eye-tracker to a smartphone via USB. For data recording, we used Pupil Mobile² and streamed the data via peer-to-peer WiFi connection to a computer running Pupil Capture³, v3.2.16. For calibration, we used the single marker calibration. For post processing, we used Pupil Player⁴, v3.2.16.

2.2 Framework for Automated Data Processing

To accelerate and simplify the data evaluation process, we developed a framework consisting of several algorithms that fully automate the evaluation process using body measures and the export of the Pupil Labs eye tracking software. All scripts are written in Python 3.7. We used pandas⁵ and NumPy⁶ for processing the data and Matplotlib⁷ and Pillow⁸ for visualization. The procedure and algorithms work exactly the same for all eye tracking data provided by Pupil Labs devices. The final framework is depicted in Figure 2, the source code can be found in our GitHub project⁹.

Extraction of Fixations. For the definition of fixations, we use the exported CSV file of Pupil Player, which lists all fixations during the recording with a normalized X and Y position, a duration, and a unique ID. We adopted the default values for fixations from the software. These were a maximum dispersion of 3.0° and a minimum duration of 300 ms.

Creating a Reference Image. Our approach for the automated processing of the recorded eye tracking data is based on the assumption that the location of specific body parts is known at all times. During a mirror exposure task with little to no movement and rotation,

¹<https://pupil-labs.com/products/core/>

²https://pupil-labs.com/blog/news/pupil_mobile/

³<https://docs.pupil-labs.com/core/software/pupil-capture/>

⁴<https://docs.pupil-labs.com/core/software/pupil-player/>

⁵<https://pandas.pydata.org/>

⁶<https://numpy.org/>

⁷<https://matplotlib.org/>

⁸<https://python-pillow.org/>

⁹<https://github.com/ChrisGoettfert/mirror-exposure-gaze-analyzer>

the position of the body parts of interest stays relatively the same over time. Thus, similar to the approach of Naumann et al. [9], we extract a single world camera image from Pupil Player as a reference picture reflecting the subject's point of view throughout the experience, see Figure 3.

Definition of AoI. Pupil Player allows defining surfaces as AoI based on Apriltag¹⁰ markers. To avoid placing markers on the body parts of our participants, we define the mirror as a singular surface using four markers, as visible in Figure 4, and developed an algorithm to define any number of separate body parts as AoI. We calculate the position of the respective body parts using eye height (height of the world camera), standard body measures for the local population, derived from ISO/TR 7250-2:2010 [5] and additional environment information, stored in a text file. The included body measures are the 50th percentile dimensions (width, length) and calculated location of the respective body part (height of the lower end of a body part). The included environment information are height of the lower edge of the lowest markers, length and width of the surface on the mirror, distance of the mirror to the ground, and distance of the subject to the mirror.

The first step in calculating AoI is a conversion from cm to px. We calculate a “scaling factor” derived from the size of our mirror and the resolution of the reference picture in px, which defines the ratio between cm and px in our reference picture. Based on this scaling factor, we can precisely locate the world camera in the reference picture and use the eye height for further calculations. The second step is the localization of body parts of interest on the reference picture. For this purpose, we developed an algorithm that can locate the body parts in the reference picture based on eye height, standard body measures and the intercept theorem, which defines the position of objects on the mirror surface.

By using Algorithm 1, we can locate the height of the body part of interest on our reference picture. By applying the same principles, the widths of the body parts can be calculated. A value that adequately describes the length of the AoI is added to the height, to obtain an appropriate length value for the AoI. To visualize the calculated AoI, bounding boxes are added to the reference picture as visible in Figure 3. For refinement of the bounding boxes, we enabled manual adjustment of their length and width.

Data Evaluation. Finally, to map the fixations to the AoI, we calculate whether the fixations were within the created bounding boxes. As mentioned earlier, each fixation has a normalized X and Y position based on the size of the surface (mirror). In the same way, we normalize the bounding box positions and calculate for each of the measured fixations whether it was inside a bounding box or not, resulting in the number of hits for each bounding box and the total duration of fixation time within a bounding box. The fixations over a certain time span can be visualized on the reference picture either with or without bounding boxes. In sum, our tool extracts the fixations from eye tracking data, combines them with a reference picture and individually defined AoI, and provides the user with information about the number of fixations and dwell time within each AoI.

ALGORITHM 1: Pseudocode to calculate the positional px height of the feet in the reference picture

Function *CalculateHeightsForAreaOfInterestPositions*

```

/* Calculate the scaling factor (px to cm
   ratio) */
scalingfactor ←  $\frac{\text{imageheight}}{\text{mirrorheight}}$ 
/* Calculate cm differences */
diffeyeheight ←  $\frac{\text{eyeheight}}{\text{feetheight}}$ 
/* Transform to px and multiply it by 0.5
   (intercept theorem) */
diffeyeheightinpx ←  $\text{diffeyeheight} \times \text{scalingfactor} \times 0.5$ 
/* Subtract differences to determine the
   height */
feetheightinpx ←  $\text{eyeheightinpx} - \text{diffeyeheightinpx}$ 

```

end

3 EVALUATION

To validate our approach, we compare the bounding boxes automatically generated by our framework using standard body measures to manually optimized bounding boxes, adjusted for each participant to the respective body parts.

3.1 Methods

Participants. The study was conducted with N = 5 participants (age: M = 23.8 years, SD = 1.94 years, 4 Female, 1 Male). All participants were either students or employees of the local university. All participants either did not have a visual impairment or had it corrected with contact lenses during the experiment. The participants' height varied from 163 cm to 174 cm.

Mirror Exposure. The mirror exposure was divided into an exploratory phase to get used to the set-up (25 s) and four guided phases (8 s each). During the guided phases, the participant was instructed to look at their head, right hand, left hand, and feet, for 8 s each. The face is the area in the reflection with the shortest distance to the eyes; the feet have the longest distance to the eyes. We added the hands as they are relatively hard to define compared to the other two areas, as they are neither connected to the floor nor the participants' height. All tasks during mirror exposure were prompted via prerecorded audio instructions.

Procedure. The experiment was performed in a laboratory of the local university. After giving consent, the participants answered a short demographic questionnaire on a computer. Then, the eye tracker was set up and calibrated three to four times using one-point calibration to achieve an optimal tracking result. The average accuracy was M = 1.46° (SD = 0.37°). The average precision was M = 0.12° (SD = 0.04°). The participant was positioned on a marker in the center of the room facing the mirror and performed the mirror exposure task.

Laboratory Setup. The laboratory setup is shown in Figure 4. We used a 50 cm x 200 cm mirror with markers attached at a height of 57 cm (lower edge) and 169 cm (upper edge). The participants stood in 1.40 m distance to the mirror and 1.40 m distance to the

¹⁰<https://april.eecs.umich.edu/software/apriltag>

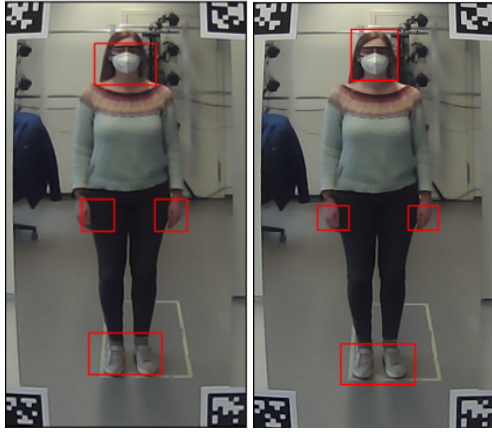


Figure 3: Reference image and AoI bounding boxes created from the framework. Left: automatically created bounding boxes, right: manually adapted bounding boxes.



Figure 4: Laboratory setup: Mirror with Apriltag markers (left), calibration marker (right), each 1.40 m distance from participant.

one point calibration marker. The calibration marker was placed at eye height for each participant individually.

Analysis of Eye Tracking Data. We defined the head (width = head width [4, 4.3.10]; length = face height $\times 1.5$ [4, 4.3.11]; vertical position = body-height - length), hands (width = hand width [4, 4.3.3]; length = hand length [4, 4.3.1]; vertical position = fist height [4, 4.4.4] + $0.5 \times$ feet length, due to gaze angle; horizontal position = center ± 0.5 hip width [4, 4.1.12]) and feet (width = $2 \times$ foot width [4, 4.3.8] + 10 cm (stance width); length = foot length [4, 4.3.7]) as AoI. Bounding boxes, fixations, and dwell time (overall duration of fixations within a bounding box) during the guided phases were calculated as described in Section 2. During the guided phases, we calculated the average distance of all measured fixations to the center of the respective calculated bounding box (error, in cm). As a measure for precision (proximity between several measures of the same type), we used the Root Mean Square (RMS) of the angular distance between successive samples (in degree) [8].

3.2 Results

Figure 3 shows the automatically created in comparison to the manually adjusted bounding boxes. Scaled by mirror size, the sizes of the automatically created bounding boxes were 22×15 cm (female) or 22×15.5 cm (male) for the head, 17×8 cm (female) or 19×8 cm (male) for each hand and 22×18 cm (female) or 23×19 cm (male) for both feet. The mean sizes (length \times width) of the manually adjusted bounding boxes were 13.6×11.28 cm for the head, 6.85×7.45 cm for each hand and 10.96×18.24 cm for both feet.

Figure 1 shows the heatmap on the mirror surface created by Pupil Labs and the automatically created bounding boxes in relation to the fixations of an exemplary participant during the mirror exposure task. While the gaze data of the phases for head and feet correspond to the respective bounding box, the automatically created bounding boxes for the hands are visibly offset. Table 1 shows the mean error, number of fixations and dwell time for each of the AoI during the guided phases for both automatically created bounding boxes (left) and manually created bounding boxes (right). While the values for hands and feet are relatively similar in both variants, the hands in the manually adjusted bounding boxes descriptively show a lower error, more fixations and longer dwell time.

4 DISCUSSION

Our work aimed to create a framework that facilitates the analysis of eye tracking data in mirror exposure. Based on a commercially available eye tracking system, we developed a framework that is easy to use and enables us to rapidly define AoI. By defining the mirror as a large surface and calculating fixations and AoI within that surface, our framework allows us to compute gaze data in mirror exposure without time-consuming post-processing. Our system can automatically calculate AoI and process and visualize gaze data based on these. Overall, the user evaluation revealed comparable results of our framework to the previous gold standard, i.e., manually defined AoI.

Our framework is not limited to the Pupil Core eye tracking glasses but can be extended to other systems. The automatic processing and openness for different systems allow a broad range of applications in real-life mirror exposures or even in virtually extended applications - an emerging treatment application [6, 10, 11, 13, 14, 16, 18]. In addition, our system allows defining and implementing any other AoI than the examples we used in our experiment. However, this requires some expertise in python, as well as a suitable selection of standard body dimensions.

However, our system still has some shortcomings. Based on the automatically created bounding boxes, manual adjustments of a few pixels still seem necessary for optimal fit. One approach to optimization would be to measure the body parts of the tested subjects. However, measuring the dimensions of each body part per person is time-consuming and intrusive - similar to attaching markers on the body. For future use, we suggest a revision of the standard dimensions used and simplifying the manual adjustments by creating a graphic user interface. Even with these manual adjustments, our method provides a time-saving approach.

Our result for hands and feet shows a relatively large error for both types of bounding boxes. Gazes to the feet were detected less accurately than the rest of the data, as the pupil tends to be covered

Table 1: Number fixations dwell times and error with automatically generated AoI. Number fixations dwell times and error with manually generated AoI.

	Automatic Bounding Boxes			Manual Bounding Boxes		
	Fixations	Dwell time (s)	Error (cm)	Fixations	Dwell time (s)	Error (cm)
	<i>M</i> (<i>SD</i>)	<i>M</i> (<i>SD</i>)	<i>M</i> (<i>SD</i>)	<i>M</i> (<i>SD</i>)	<i>M</i> (<i>SD</i>)	<i>M</i> (<i>SD</i>)
Head	14.0 (4.86)	3.6 (1.26)	5.5 (2.02)	12.6 (4.22)	3.1 (1.09)	6.6 (2.18)
Left hand	7.4 (5.39)	1.8 (1.22)	5.2 (2.07)	8.4 (5.08)	2.1 (1.10)	4.7 (1.61)
Right hand	4.4 (3.83)	1.0 (0.99)	8.8 (3.08)	7.6 (4.22)	2.0 (1.10)	8.1 (4.25)
Feet	2.0 (2.10)	0.4 (0.42)	18.7 (8.67)	3.6 (2.80)	0.8 (0.68)	18.3 (9.93)

when looking downwards and the feet are furthest to the eye position. The bounding boxes created for the hands are comparatively small which makes them vulnerable to small, idle body movements of the participants, to the participants not standing exactly in the center of the mirror and to the overall tracking accuracy. The current framework bases on the premise that there is no body motion during the mirror exposure. Future work could solve this problem via a human pose estimation algorithms using deep learning methods like OpenPose [3] that track different body parts in real-time. This way, AoI could be analyzed in motion.

5 CONCLUSION

We have presented a framework that enables simple and fast processing and analyses of eye tracking data during mirror exposure tasks. Taking eye tracking system from Pupil Labs as an example, we have developed an algorithm that allows us to automatically define areas of interest, manually optimize them, and evaluate and visualize gaze data. Our system allows easy to use application in various fields of research on mirror exposure.

ACKNOWLEDGMENTS

This research has been funded by the German Federal Ministry of Education and Research in the project ViTraS (16SV8219).

REFERENCES

- [1] Rike Arkenau, Anika Bauer, Silvia Schneider, and Silja Vocks. 2022. Gender differences in state body satisfaction, affect, and body-related attention patterns towards one's own and a peer's body: an Eye-Tracking Study with Women and Men. *Cognitive Therapy and Research* 46, 4 (2022), 1–12. <https://doi.org/10.1007/s10608-022-10300-5>
- [2] Anika Bauer, Silvia Schneider, Manuel Waldorf, Karsten Braks, Thomas J Huber, Dirk Adolph, and Silja Vocks. 2017. Selective visual attention towards oneself and associated state body satisfaction: an eye-tracking study in adolescents with different types of eating disorders. *Journal of abnormal child psychology* 45, 8 (2017), 1647–1661. <https://doi.org/10.1007/s10802-017-0263-z>
- [3] Zhe Cao, Tomas Simon, Shih-En Wei, and Yaser Sheikh. 2017. Realtime Multi-person 2D Pose Estimation Using Part Affinity Fields. In *2017 IEEE Conference on Computer Vision and Pattern Recognition (CVPR)*. 1302–1310. <https://doi.org/10.1109/CVPR.2017.143>
- [4] DIN CEN ISO/TR 7250-2:2013-08 2013. *Basic human body measurements for technological design - Part 2: Statistical summaries of body measurements from national populations (ISO/TR 7250-2:2010 + Amd 1:2013); German version CEN ISO/TR 7250-2:2011 + A1:2013*. Standard. <https://doi.org/10.31030/1935074>
- [5] DIN EN ISO 7250-1:2017-12 2017. *Basic human body measurements for technological design - Part 1: Body measurement definitions and landmarks (ISO 7250-1:2017); German version EN ISO 7250-1:2017*. Standard. <https://doi.org/10.31030/2778667>
- [6] Nina Döllinger, Erik Wolf, David Mal, Stephan Wenninger, Mario Botsch, Marc Erich Latoschik, and Carolin Wienrich. 2022. Resize me! Exploring the user experience of embodied realistic modifiable avatars for body image intervention in virtual reality. *arXiv* (2022), 1–36. <https://doi.org/10.48550/arXiv.2203.05060>
- [7] Trevor C Griffen, Eva Naumann, and Tom Hildebrandt. 2018. Mirror exposure therapy for body image disturbances and eating disorders: A review. *Clinical Psychology Review* 65 (2018), 163–174. <https://doi.org/10.1016/j.cpr.2018.08.006>
- [8] Moritz Kassner, William Patera, and Andreas Bulling. 2014. Pupil: An Open Source Platform for Pervasive Eye Tracking and Mobile Gaze-based Interaction. In *Adjunct Proceedings of the 2014 ACM International Joint Conference on Pervasive and Ubiquitous Computing (Seattle, Washington) (UbiComp '14 Adjunct)*. ACM, New York, NY, USA, 1151–1160. <https://doi.org/10.1145/2638728.2641695>
- [9] Eva Naumann, Stefanie Biehl, and Jennifer Svaldi. 2019. Eye-tracking study on the effects of happiness and sadness on body dissatisfaction and selective visual attention during mirror exposure in bulimia nervosa. *International Journal of Eating Disorders* 52, 8 (2019), 895–903. <https://doi.org/10.1002/eat.23127>
- [10] Bruno Porras-García, Marta Ferrer-García, Lena Yilmaz, Yigit O Sen, Agata Olszewska, Alexandra Ghita, Eduardo Serrano-Troncoso, Janet Treasure, and José Gutiérrez-Maldonado. 2020. Body-related attentional bias as mediator of the relationship between body mass index and body dissatisfaction. *European Eating Disorders Review* 28, 4 (2020), 454–464.
- [11] Bruno Porras-García, Alexandra Ghiță, Manuel Moreno, Marta Ferrer García Ferrer, Paola Bertomeu Panisello, Eduardo Serrano Troncoso, Giuseppe Riva, Antonios Dakanalis, Jose Achotegui-Loizate, Antoni Talarn-Caparrós, et al. 2018. Gender differences in attentional bias after owning a virtual avatar with increased weight. *Annual Review of CyberTherapy and Telemedicine*, 2018 16 (2018), 73–79.
- [12] Cristina González Sánchez, Sandra Díaz Ferrer, José Alejandro Aristizabal Cuellar, José Luis Mata Martín, and Sonia Rodríguez Ruiz. 2022. I Look at my whole body and i feel better: attentional bias, emotional and psychophysiological response by pure exposure treatment in women with obesity. *Psychotherapy Research* 0, 0 (2022), 1–15. <https://doi.org/10.1080/10503307.2021.2021310>
- [13] Anne Thaler. 2019. *The Role of Visual Cues in Body Size Estimation*. Vol. 56. Logos Verlag Berlin GmbH, Berlin.
- [14] Anne Thaler, Ivelina V Piryanikova, Jeanine K Stefanucci, Sergi Pujades, Stephan de la Rosa, Stephan Streuber, Javier Romero, Michael J Black, and Betty J Mohler. 2018. Visual Perception and Evaluation of Photo-Realistic Self-Avatars From 3D Body Scans in Males and Females. *Frontiers in ICT* 5 (2018), 18. <https://doi.org/10.3389/fict.2018.00018>
- [15] Brunna Tuschen-Caffier, Caroline Bender, Detlef Caffier, Katharina Klenner, Karsten Braks, and Jennifer Svaldi. 2015. Selective visual attention during mirror exposure in anorexia and bulimia nervosa. *PLOS one* 10, 12 (2015), e0145886. <https://doi.org/10.1371/journal.pone.0145886>
- [16] Erik Wolf, Marie Luisa Fiedler, Nina Döllinger, Carolin Wienrich, and Marc Erich Latoschik. 2022. Exploring Presence, Avatar Embodiment, and Body Perception with a Holographic Augmented Reality Mirror. In *2022 IEEE Conference on Virtual Reality and 3D User Interfaces (VR)*. 350–359. <https://doi.org/10.1109/VR51125.2022.00054>
- [17] Erik Wolf, Ronja Heinrich, Annabell Michalek, David Schraudt, Anna Hohm, Rebecca Hein, Tobias Grundgeiger, and Oliver Happel. 2019. Rapid Preparation of Eye Tracking Data For Debriefing In Medical Training: A Feasibility Study. *Proceedings of the Human Factors and Ergonomics Society Annual Meeting* 1 (2019), 733–737. <https://doi.org/10.1177/1071181319631032>
- [18] Erik Wolf, Nathalie Merdan, Nina Döllinger, David Mal, Carolin Wienrich, Mario Botsch, and Marc Erich Latoschik. 2021. The Embodiment of Photorealistic Avatars Influences Female Body Weight Perception in Virtual Reality. In *2021 IEEE Virtual Reality and 3D User Interfaces (VR)*. 65–74. <https://doi.org/10.1109/VR50410.2021.00027>
- [19] World Health Organization. 2019. *International statistical classification of diseases and related health problems (11th ed.)*. World Health Organization. <https://icd.who.int/>